Ab Initio Study of the Structure and Polarizability of Sulfur Clusters, S_n ($n = 2-12$)

S. Millefiori* and A. Alparone

Dipartimento di Scienze Chimiche, Università di Catania, Viale A. Doria 8, 95125 Catania, Italy

Received: June 5, 2001; In Final Form: August 9, 2001

The structure and the dipole polarizabilities of S_n clusters ($n = 2-12$) have been calculated using density functional theory within the B3LYP approximation and conventional ab initio Hartree−Fock (HF) and coupled-cluster with single and double and perturbative triple excitations (CCSD(T)) methods. The results show that the binding energy per atom increases with the size of the cluster and reaches the asymptotic limit for a relatively small n value. There is an excellent agreement between B3LYP and CCSD(T) data in predicting the energy of the disproportionation reaction $2S_n \rightarrow S_{n-1} + S_{n+1}$, which indicates that S_2, S_6, and S_8 are especially stable, in agreement with the experiment. $\langle\alpha\rangle$ increases with n and linearly correlates with the molecular volume. $\langle\alpha\rangle/n$ increases with n and reaches the asymptotic limit per $n \rightarrow \infty$ from below, contrary to what happens in small semiconductor and metallic clusters. A well-defined correlation between $\langle\alpha\rangle$ and hardness is not found, while the $\langle\alpha_n\rangle - n\langle\alpha_1\rangle$ difference value linearly correlates with the atomization energy. In the sulfur clusters, the minimum polarizability principle does not hold, the lone-pair electron polarizability being more diffuse, hence more polarizable, in the cluster than in the free atom. Pure vibrational effects on $\langle\alpha\rangle$ are negligible.

1. Introduction

The static dipole polarizability, α, is a fundamental property of a molecule and governs a variety of physical and chemical phenomena.[1] It expresses the induced dipole moment value of the molecule under the effect of a weak external field.[2] Thus, it can be taken as a measure of the stability of the electronic distribution. The minimum polarizability principle (MPP)[3,4] was indeed formulated, which states that "the natural evolution of any system is toward a state of minimum polarizability". This implies $\langle\alpha_M\rangle < \sum_i\langle\alpha_i\rangle$, where $\langle\alpha_M\rangle$ is the molecular mean dipole polarizability and $\langle\alpha_i\rangle$ is the mean polarizability of the constituent fragment. However, the MPP does not always hold.[5] The reasons are not fully understood. The MPP is conceptually related to the maximum hardness principle (MHP)[6] based on the absolute hardness definition[2]

$$\eta = \frac{1}{2}\left(\frac{\partial^2 E}{\partial N^2}\right)_v \cong \frac{1}{2}(I - A) \cong \frac{1}{2}(\epsilon_{LUMO} - \epsilon_{HOMO})$$

where N is the number of electrons and I and A are the ground-state ionization potential and electron affinity, respectively. According to the η definition, molecules arrange themselves so as to be as hard as possible. Maximum hardness, minimum polarizability, and molecular stability complement each other.[7−9] Concepts underlying MPP and MHP definitions have been often used in the literature to study a variety of chemical reactions[5−10] including hydrogen-bonded complexes,[8] tautomeric equilibria,[11] internal rotations,[7,12] and relative stability of isomers.[13] Relationships among polarizability, dipole moment,[14] and electronic excitations[15] have been also reported. Correlation between hardness and polarizability has been investigated for atoms, molecules, and homonuclear clusters.[12,16] As recent examples, in furan homologues,[17,18] α, as well as the first hyperpolarizability, β, and the second hyperpolarizability, γ, linearly decreases as η increases, pure electronic contributions having been considered because vibrational contributions are small.[19] Similar trends were observed in the group 14 heterocyclic series $C_4H_4XH_2$ (X = C, Si, Ge, Sn).[20] In many cases, however, no correlation has been found between α and η; in a series of molecules containing the atoms H, C, N, O, S, P, F, Cl, Br, I, Fe, and Os[5] and in the group 16 chalcogenophenes C_4H_4X (X = O, S, Se, Te),[17] the dipole polarizability difference

$$\delta\alpha = \langle\alpha_M\rangle - \sum_i\langle\alpha_i\rangle$$

was found to be linearly related to the molecular stability expressed as binding energy, $BE = E_M - \sum_i E_i$. On the whole, it can be stated that the interrelation between α and the chemical stability is not straightforward, leaving some lack of knowledge on the effective role of the microscopic properties associated with the molecular dipole polarizability.

The present work aims to investigate the size dependence of the dipole polarizability and stability of mainly cyclic sulfur clusters, S_n ($n = 2-12$), and the possible correlation among electronic properties in these systems. Theoretical methods are used within the conventional ab initio and density functional theory (DFT) framework. These clusters are characterized by the presence of many polarizable lone-pair electrons, which likely dominate the molecular polarizability.

The chemistry of elemental sulfur has attracted much attention owing to the richness of molecular forms it shows.[21] In the vapor, the molecules S_2 to S_{10} are known. They have been characterized experimentally by X-ray, IR, Raman, and UV absorption spectroscopies, as well as by theoretical calculations.[22−26] Dipole polarizabilities of cyclic S_8, S_{12}, S_{16}, and S_{20}, evaluated at the semiempirical MNDO level, have been recently reported.[27]

* To whom correspondence should be addressed. E-mail: smillefiori@dipchi.unict.it. Fax: +39 095 580138.

10.1021/jp0121466 CCC: $20.00
Published on Web 09/21/2001

2. Computational Methods

All theoretical calculations were made with the Gaussian 98 package.[28] Molecular geometries were optimized at Hartree−Fock (HF) and DFT-B3LYP levels using the correlation consistent cc-pVDZ basis set.[29] Moeller-Plesset second-order perturbation theory (MP2) and coupled-cluster with single and double and perturbative triple excitations (CCSD(T)) single point energy and polarizability calculations were carried out on the B3LYP/cc-pVDZ geometry for $n = 2-10$ and $n = 2-7$, respectively.

A vibrational analysis was performed to discriminate between minima and transition states in the potential energy surface (PES). IR and Raman frequencies were obtained analytically. The HF and B3LYP components of the static electronic dipole polarizability were obtained analytically as the second derivatives of the energy with respect to the Cartesian components of the electric field:

$$\alpha_{ij} = -\left[\frac{\partial^2 E}{\partial F_i\, \partial F_j}\right]_{F=0}$$

MP2 and CCSD(T) α_{ij} terms were obtained numerically from a Taylor expansion of the cluster energy, E, in the electric field, F:

$$E(F) = E(0) - \sum_i \mu_i F_i - \frac{1}{2}\sum_{ij} \alpha_{ij} F_i F_j - \ldots$$

using a field strength of 0.005 au within the finite field method as developed by Kurtz et al.[30]

Vibrational contributions to the polarizability were evaluated in the double harmonic approximation following summation over mode expression:

$$\alpha_{ij}^{v} = [\mu^2]^{0,0} = \sum_a^{3N-6} \frac{\left(\frac{\partial \mu_i^e}{\partial Q_a}\right)_0 \left(\frac{\partial \mu_j^e}{\partial Q_a}\right)_0}{\omega_a{}^2}$$

where the symbols have their usual meaning.[31]

The mean polarizability $\langle\alpha\rangle$ is reported as

$$\langle\alpha\rangle = \frac{1}{3}(\alpha_{xx} + \alpha_{yy} + \alpha_{zz})$$

and the polarizability anisotropy is reported as

$$\Delta\alpha = \left\{\frac{1}{2}[(\alpha_{xx} - \alpha_{yy})^2 + (\alpha_{xx} - \alpha_{zz})^2 + (\alpha_{yy} - \alpha_{zz})^2]\right\}^{1/2}$$

3. Results and Discussion

3.1. Cluster Structure and Stability. The B3LYP/cc-pVDZ molecular structures of the clusters investigated are reported in Figure 1, and their geometrical parameters are reported in Table 1. For $n \geq 5$, we have considered only cyclic structures because these clusters occur as monocyclic rings.[21] S_2 has a $^3\Sigma_g^-$ ground state with a bond length of 1.934 Å and a vibrational frequency of 702 cm^{-1}. Both of these figures are in reasonable agreement with the corresponding experimental values of 1.889 Å and 726 cm^{-1}.[32]

S_3 and S_4 clusters have been investigated in some detail because their PES is rather flat and because many valuable theoretical computations exist in the literature for comparison.[23−25,33−39] The experimental structure of S_3 is not known;

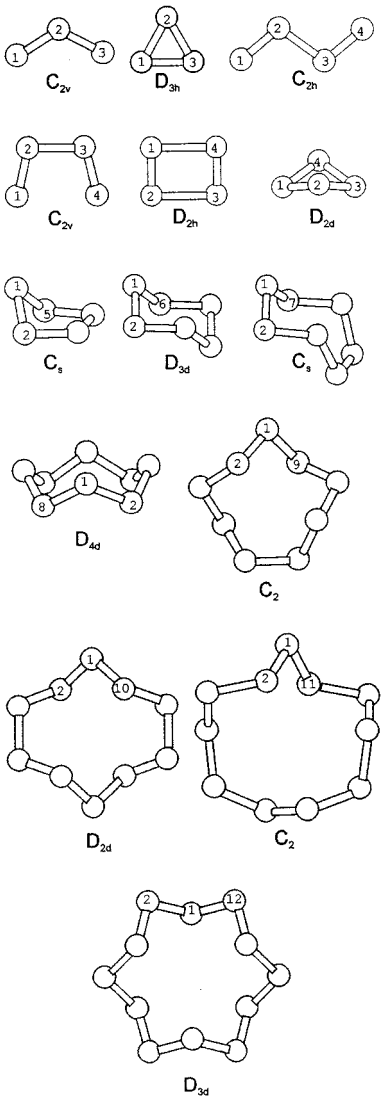

Figure 1. Ground-state structures of S_n clusters.

nevertheless the S−S bond length was estimated to be 1.90 ± 0.05 Å.[40] We know the ionization potential (9.68 eV),[41] the electron affinity (2.093 ± 0.025 eV),[40] and the absorption in the visible region (λ_{max} = 430 nm).[42] Earlier correlated methods predicted the open C_{2v} structure to be more stable than the ring D_{3h} form by 5−10 kcal/mol. The C_{2v} structure is compatible with the vibrational spectrum.[43] The B3LYP/aug-cc-pVDZ results (Table 2) indicate the C_{2v} form as the global minimum with the D_{3h} form being 8.14 kcal/mol less stable, which are in agreement with the DFT results of Goddard et al.[38] and with those obtained with the multireference configuration interaction (CI) method,[37] and are corroborated by the present CCSD(T)/aug-cc-pVDZ//B3LYP/cc-pVDZ calculations. The C_{2v} ($^3A_2$) form is less stable by 14.37 kcal/mol in agreement with the results by Hohl et al.,[23] which found the lowest energy triplet state 16−18 kcal/mol above the ground state. As to the C_{2v} molecular geometry, the B3LYP/cc-pVDZ calculations predict a S−S bond length of 1.960 Å and a bond angle of 117.5° in very good agreement with the results of previous ab initio correlated and multireference calculations: 1.948 Å (MP2),[24] 1.951 Å (MRCI/DZP),[35] and 1.932 Å (CCSD(T)),[37] the bond angle being, in every case, in the small 117−118° range. Thus, despite its single-reference character, the B3LYP method adequately describes the structure and PES of S_3.

TABLE 1: B3LYP/cc-pVDZ Optimized Geometries of S_n Clusters[a]

		parameter	calcd	exptl
S_2	($D_{\infty h}$, $^3\Sigma_g^-$)	r(1−2)	1.934	
S_3	(D_{3h}, $^1A_1'$)	r(1−2)	2.127	
	(C_{2v}, $^1A_1$)	r(1−2)	1.960	
		θ(1−2−3)	117.5	
	(C_{2v}, $^3A_2$)	r(1−2)	2.033	
		θ(1−2−3)	94.2	
S_4	(D_{2d}, $^1A_1$)	r(1−2)	2.168	
		θ(1−2−3)	85.2	
		ϕ(1−2−3−4)	32.3	
	(D_{2h}, ^1A_g)	r(1−2)	1.926	
		r(1−4)	2.604	
	(C_{2v}, $^1A_1$)	r(1−2)	1.939	
		r(2−3)	2.230	
		θ(1−2−3)	103.6	
	(C_{2v}, $^3B_2$)	r(1−2)	1.930	
		r(2−3)	2.722	
		θ(1−2−3)	93.7	
	(C_{2h}, ^1A_g)	r(1−2)	1.960	
		r(2−3)	2.137	
		θ(1−2−3)	110.4	
S_5	(C_s, $^1A'$)	r(1−2)	2.133	
		r(2−3)	2.072	
		r(3−4)	2.248	
		θ(5−1−2)	90.5	
		θ(1−2−3)	99.9	
		θ(2−3−4)	100.9	
		ϕ(5−1−2−3)	63.3	
		ϕ(1−2−3−4)	−39.8	
S_6	(D_{3d}, $^1A_{1g}$)	r(1−2)	2.120	2.068
		θ(1−2−3)	102.5	102.6
		ϕ(1−2−3−4)	74.0	73.8
S_7	(C_s, $^1A'$)	r(1−2)	2.099	2.048
		r(2−3)	2.165	2.090
		r(3−4)	2.031	1.998
		r(4−5)	2.262	2.175
		θ(7−1−2)	106.5	105.0
		θ(1−2−3)	102.4	102.1
		θ(2−3−4)	106.6	105.3
		θ(3−4−5)	108.0	107.4
		ϕ(7−1−2−3)	76.4	76.7
		ϕ(1−2−3−4)	−106.1	−107.8
		ϕ(2−3−4−5)	82.2	83.2
S_8	(D_{4d}, $^1A_1$)	r(1−2)	2.108	2.055
		θ(1−2−3)	108.3	108.2
		ϕ(1−2−3−4)	98.4	98.5
S_9	(C_2, ^1A)	r(1−2)	2.116	
		r(2−3)	2.094	
		r(3−4)	2.131	
		r(4−5)	2.109	
		r(5−6)	2.117	
		θ(9−1−2)	104.0	
		θ(1−2−3)	110.1	
		θ(2−3−4)	108.1	
		θ(3−4−5)	107.0	
		θ(4−5−6)	108.2	
		ϕ(9−1−2−3)	74.9	
		ϕ(1−2−3−4)	−76.1	
		ϕ(2−3−4−5)	−62.5	
		ϕ(3−4−5−6)	113.7	
		ϕ(4−5−6−7)	−85.7	
S_{10}	(D_{2d}, ^1A)	r(1−2)	2.104	2.048
		r(2−3)	2.130	2.074
		r(3−4)	2.094	2.035
		θ(10−1−2)	112.1	110.2
		θ(1−2−3)	105.0	103.4
		θ(2−3−4)	106.9	107.1
		ϕ(10−1−2−3)	79.2	78.6
		ϕ(1−2−3−4)	−122.0	−122.6
		ϕ(2−3−4−5)	75.9	76.1
S_{11}	(C_2, ^1A)	r(1−2)	2.109	2.046
		r(2−3)	2.114	2.065
		r(3−4)	2.100	2.046
		r(4−5)	2.133	2.064
		r(5−6)	2.088	2.037
		r(6−7)	2.155	2.110
		θ(11−1−2)	104.0	103.8
		θ(1−2−3)	106.8	104.6
		θ(2−3−4)	108.2	105.4
		θ(3−4−5)	108.5	106.9
		θ(4−5−6)	109.8	107.6
		θ(5−6−7)	108.7	106.3
		ϕ(11−1−2−3)	89.1	91.5
		ϕ(1−2−3−4)	−72.3	−71.5
		ϕ(2−3−4−5)	−83.0	−82.0
		ϕ(3−4−5−6)	116.5	115.0
		ϕ(4−5−6−7)	−103.1	−104.0
		ϕ(5−6−7−8)	134.0	140.0
S_{12}	(D_{3d}, $^1A_{1g}$)	r(1−2)	2.111	2.052
		θ(12−1−2)	107.3	106.0
		θ(1−2−3)	107.8	107.2
		ϕ(1−2−3−4)	87.5	88.0

[a] r = bond length (Å), θ = bond angle (deg), ϕ = dihedral angle (deg).

In the case of S_4, we have considered four isomers with D_{2d}, D_{2h}, C_{2v}, and C_{2h} symmetry. They all are minima in the B3LYP/cc-pVDZ PES, except the rectangular D_{2h} form, which is a transition state. The experimental molecular geometry of S_4 is not known. IR spectra of sulfur vapor[44] gave evidence for the presence of two different S_4 open-chain structural isomers. Earlier theoretical studies indicated that at MRCI,[25,45] CCSD(T),[25] MD-DF,[46] and QCISD(T)[47] levels the two most stable isomers are the planar cis and the rectangular D_{2h} forms, the former being slightly favored, while MP2, MP4,[24] and MD-DF[23] calculations predicted the D_{2h} isomer to be the global minimum. Our B3LYP/aug-cc-pVDZ//B3LYP/cc-pVDZ data agree with the former results and with those of very recent BLYP/CEP-121(BPF) and BLYP/6-31G(BPF) calculations[48] by predicting the C_{2v} ($^1A_1$) cis planar form of S_4 to be the ground state and putting the D_{2h}, cis C_{2v} ($^3B_2$), C_{2h}, and D_{2d} structures 2.11, 2.18, 6.89, and 17.99 kcal/mol higher in energy (Table 2). CCSD(T)/aug-cc-pVDZ//B3LYP/cc-pVDZ calculations indicate that the D_{2h} and C_{2v} ($^1A_1$) isomers are practically isoenergetic. The cis C_{2v} ($^3B_2$) is a local minimum lying 6.02 kcal/mol above the ground state, in agreement with the MD-DF results of Hohl et al.[23] Compared with the recent QCISD(T)/6-311G(d) results, the B3LYP/aug-cc-pVDZ geometrical parameters appear to be somewhat overestimated, as expected, by 0.088 and 0.09 Å for r_{1-2} and r_{2-3}, respectively.

The optimized ground-state structures of S_5−S_{12} are reported in Table 1, together with the available experimental data. X-ray structures are known for S_6,[49] S_7,[50] S_8,[51] S_{10},[52] S_{11},[53] and S_{12}.[54] The B3LYP/cc-pVDZ calculations correctly reproduce the cluster configuration. Bond distances are systematically over-

TABLE 2: Total, E_T (au), and Relative , E_R (kcal/mol), Energy of S_n Clusters

		B3LYP/aug-cc-pVDZ// B3LYP/cc-pVDZ			CCSD(T)/aug-cc-pVDZ// B3LYP/cc-pVDZ	
		E_T	E_R	E_R[a]	E_T	E_R
S_1		−398.127 993			−397.610 557	
S_2		−796.410 899			−795.354 760	
S_3	(C_{2v}, $^1A_1$)	−1194.617 558	0.00	0.00	−1193.036 164	0.00
	(D_{3h}, $^1A_1'$)	−1194.604 584	8.14	7.35	−1193.022 859	8.35
	(C_{2v}, $^3A_2$)	−1194.594 663	14.37	14.12	−1193.006 628	18.53
S_4	(C_{2v}, $^1A_1$)	−1592.837 190	0.00	0.00	−1590.730 807	0.16
	(D_{2h}, ^1A_g)	−1592.833 825	2.11	1.26	−1590.731 063	0.00
	(C_{2v}, $^3B_2$)	−1592.833 723	2.18	0.52	−1590.721 468	6.02
	(C_{2h}, ^1A_g)	−1592.826 213	6.89	7.47	−1590.716 081	9.40
	(D_{2d}, $^1A_1$)	−1592.808 527	17.99	18.80	−1590.701 832	18.34
S_5		−1991.067 597			−1988.432 966	
S_6		−2389.301 915			−2386.141 527	
S_7		−2787.522 759			−2783.834 275	
S_8		−3185.753 024				
S_9		−3583.960 175				
S_{10}		−3982.180 001				
S_{11}		−4380.398 901				
S_{12}		−4778.625 470				

[a] B3LYP/cc-pVDZ//B3LYP/cc-pVDZ results.

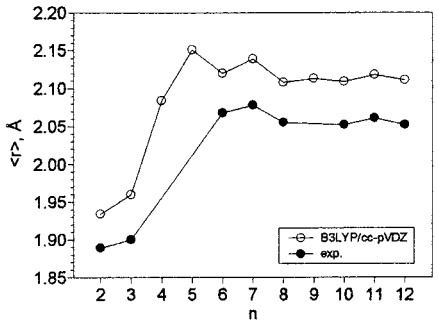

Figure 2. Calculated and experimental average S−S bond length as a function of the S_n cluster size.

estimated by ca. 0.05 Å. Bond and dihedral angles are satisfactorily reproduced (to within 2°), the most difficult case being S_{11} for which $\Delta\phi(5-6-7-8)$ is ca. 6°.

Figure 2 shows the average S−S bond length, $\langle r \rangle$, variation with the cluster size. For smaller clusters ($n = 2-4$), which have an open structure, $\langle r \rangle$ reflects a greater double bond contribution. As the cluster size increases, $\langle r \rangle$ rapidly converges to the asymptotic limit, showing a clear even−odd alternation, which well reproduces the experimental behavior. Figure 2 also suggests that even-membered clusters should be more stable than their odd-membered neighbors.

The absolute energies of the S_5-S_{12} clusters are listed in Table 2, while Figure 3 shows the evolution of the binding energy per atom, BE/*n*. The results indicate that a great part of the cohesion energy is due to the electron correlation, the DFT-B3LYP approach somewhat overestimating BE with respect to the MP2 and CCSD(T) methods. For smaller clusters, BE monotonically increases from S_2 to S_6 and then smoothly converges to the extrapolated limit value for $n \rightarrow \infty$ of 2.56 (MP2) and 2.67 (B3LYP) eV, which compares well with the experimental value of 2.74 eV,[21] the asymptotic limit being obtained by fitting the property to an inverse polynomial of the form $BE/n = a + b/n + c/n^2$. Thus, in these compact types of clusters, the cohesive energy in the solid appears to be reached for a relatively small *n* value. The same behavior was found by DFT calculations in Si_n clusters.[55] It is of interest to note that the cohesive energy of Si in the bulk, 4.63 eV,[56] is about 2 times the S_∞ figure.

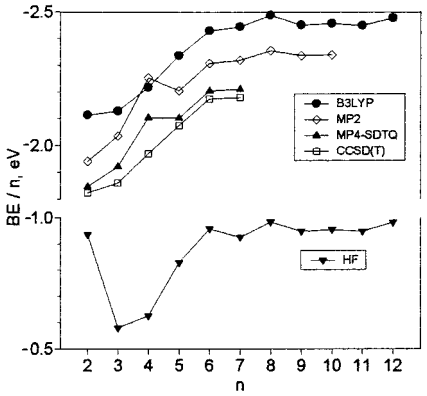

Figure 3. Binding energy per atom as a function of the S_n cluster size. Basis set is aug-cc-pVDZ.

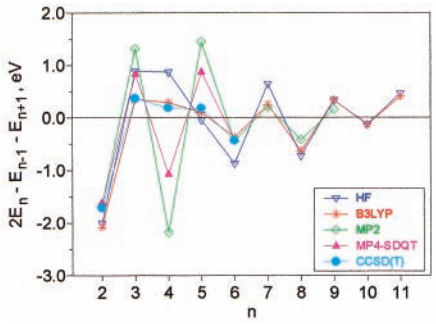

Figure 4. Disproportionation energy as a function of the S_n cluster size. Basis set is aug-cc-pVDZ.

The monotonic increase of BE with *n* suggests that the cluster is stable toward the fragmentation reaction

$$S_n \rightarrow S_{n-1} + S$$

whereas the energy of the disproportionation reaction

$$2S_n \rightarrow S_{n+1} + S_{n-1}$$

which is a sensitive quantity reflecting the local stability of the cluster and can be compared to the experimental relative abundance, shows that S_2, S_6, and S_8 clusters are especially stable, in agreement with the experiment[21,57] (Figure 4). MP2 and MP4, but not CCSD(T), calculations confer a pronounced relative stability also to S_4. Indeed, mass spectroscopy studies on the fragmentation process of chalcogen microclusters[57] provided evidence for sizable production of S_4^+. Furthermore, at 450° and 20 Torr, S_4 is assumed to account for about 20% of the sulfur vapor.[57] It is remarkable that B3LYP results are in excellent agreement with the CCDS(T) ones.

3.2. Polarizabilities. Table 3 reports $\langle\alpha\rangle$ and $\Delta\alpha$ values of S_n clusters obtained by correlated methods using the diffuse aug-cc-pVDZ basis set. The best results refer to CCSD(T) calculations, which are known to give accurate values of atomic[58] and molecular[59] polarizabilities and hyperpolarizabilities. An indication of the accuracy of the calculated $\langle\alpha\rangle$ values is provided by the comparison between the CCSD(T) (18.1 au) and B3LYP (18.5 au) and the most recent experimental $\langle\alpha\rangle$ value of the S atom of 19.6 au.[60] From the methodological point of view, it is of interest to investigate the basis set effect on the calculated properties of homonuclear clusters because it has been often reported in the literature that in oligomeric compounds the enlargement of the basis set is less and less important as the size of the oligomer increases.[61] Our results for the S_n clusters are reported in Table 4 and diagrammatically shown in

TABLE 3: Calculated Mean Static Dipole Polarizability, ⟨α⟩ (au), and Polarizability Anisotropy, Δα (au), of S_n Clusters[a]

		B3LYP		MP2		MP3		MP4-DQ		MP4−SDQ		MP4−SDTQ		CCSD		CCSD(T)	
		⟨α⟩	Δα	⟨α⟩	Δα	⟨α⟩	Δα	⟨α⟩	Δα	⟨α⟩	Δα	⟨α⟩	Δα	⟨α⟩	Δα	⟨α⟩	Δα
S_1		18.50	4.09	17.92	3.91	17.97	4.11	17.98	4.15	17.99	4.15	18.04	4.18	18.02	4.18	18.10	4.26
S_2		40.10	29.22	38.23	24.60	39.02	27.05	39.46	28.14	39.93	29.36	39.52	27.81	40.73	31.36	40.53	30.39
S_3	(D_{3h}, $^1A_{1'}$)	57.72	19.77	57.54	19.62	57.07	19.84	57.21	19.94	57.37	19.90	57.68	19.57	57.39	19.82	57.65	19.66
	(C_{2v}, $^1A_1$)	68.70	66.49	64.10	52.92	67.70	64.62	70.51	72.50	71.02	73.48	67.41	61.79	70.72	72.49	69.33	67.55
	(C_{2v}, $^3A_2$)	71.66	62.34	83.41	99.75	81.56	94.88	81.42	94.23	75.57	76.78	74.88	73.89	72.24	64.31	70.87	58.78
S_4	(C_{2v}, $^3B_2$)	93.15	64.55	78.58	46.24	84.51	46.22	86.51	46.22	90.66	55.70	85.02	46.19	94.71	66.58	92.55	60.84
	(C_{2h}, ^1A_g)	111.39	85.58											117.72	94.15	123.97	104.12
	(D_{2d}, $^1A_1$)	78.85	27.78	78.44	27.05	77.52	26.96	77.64	27.12	77.99	27.21	78.61	27.02	78.05	27.24	78.61	27.15
	(C_{2v}, $^1A_1$)	94.34	72.30											96.09	74.66	100.23	85.40
S_5		103.34	37.70	102.14	35.70	99.82	34.43	99.91	34.49	101.01	35.32	102.76	36.16	101.50	35.89	103.28	36.97
S_6		124.16	53.40	122.92	50.55	120.56	49.15	120.57	49.20	121.71	50.22	123.56	51.16	122.00	50.62	123.79	51.76
S_7		152.94	33.40	151.25	31.90												
S_8		179.01	92.85	176.34	87.46												
S_9		199.81	76.60	196.13	70.79												
S_{10}		228.38	100.64	223.43	92.74												

[a] All the calculations are carried out on the B3LYP/cc-pVDZ geometries with the aug-cc-pVDZ basis set.

TABLE 4: Dependence on the Basis Set of the Mean Static Dipole Polarizability, ⟨α⟩ (au), and Polarizability Anisotropy, Δα (au), of S_n Clusters[a]

			HF		B3LYP			HF		B3LYP	
basis set			⟨α⟩	Δα	⟨α⟩	Δα		⟨α⟩	Δα	⟨α⟩	Δα
cc-pVDZ	S_1		8.40	0.89	8.27	0.59	S_5	76.81	40.70	79.29	42.51
aug-cc-pVDZ			17.74	3.35	18.50	4.09		97.31	34.68	103.34	37.70
d-aug-cc-pVDZ			19.05	3.62	20.51	4.53		98.83	34.95	105.29	37.72
cc-pVTZ			12.46	0.35	12.49	0.55					
aug-cc-pVTZ			18.86	3.27	20.12	4.04					
cc-pVDZ	S_2		30.99	47.66	27.01	35.69	S_6	94.04	52.34	96.64	55.38
aug-cc-pVDZ			42.76	38.40	40.10	29.22		117.71	49.09	124.16	53.40
d-aug-cc-pVDZ			44.08	37.98	41.83	28.81		119.07	48.90	125.92	52.96
cc-pVTZ			36.28	43.82	33.05	33.90					
aug-cc-pVTZ			44.05	37.89	41.79	28.90					
cc-pVDZ	S_3	(D_{3h}, $^1A_{1'}$)	43.28	34.40	41.81	31.36	S_7	115.74	31.25	120.82	34.56
aug-cc-pVDZ			56.91	22.33	57.72	19.77		143.18	20.05	152.94	33.40
d-aug-cc-pVDZ			58.61	22.82	60.22	20.10		144.66	30.03		
cc-pVTZ			49.89	29.66	49.54	27.89					
aug-cc-pVTZ			59.98	20.26	59.98	20.26					
cc-pVDZ		(C_{2v}, $^1A_1$)	56.01	87.31	50.26	69.46	S_8	134.95	78.19	142.71	88.41
aug-cc-pVDZ			72.78	81.15	68.70	66.49		166.43	80.65	179.01	92.85
d-aug-cc-pVDZ			74.49	80.79	70.60	65.84		167.91	80.09		
cc-pVTZ			63.81	84.57	58.84	68.77					
aug-cc-pVTZ			74.45	80.47	70.55	65.83					
cc-pVDZ		(C_{2v}, $^3A_2$)	58.13	80.60	53.54	66.61	S_9	150.40	60.31	160.06	71.73
aug-cc-pVDZ			73.45	72.45	71.66	62.34		184.75	63.81	199.81	76.60
d-aug-cc-pVDZ			75.30	72.25	73.73	61.78		186.27	63.41		
cc-pVTZ			63.97	73.92	62.40	66.49					
aug-cc-pVTZ			74.49	70.03	73.87	62.46					
cc-pVDZ	S_4	(D_{2d}, $^1A_1$)	60.18	39.75	58.85	37.41	S_{10}	171.26	79.37	183.71	94.28
aug-cc-pVDZ			77.04	29.46	78.85	27.78		209.73	83.66	228.38	100.64
d-aug-cc-pVDZ			78.71	29.94	81.18	28.06		211.32	83.11		
cc-pVDZ		(C_{2v}, $^1A_1$)	93.30	131.66	72.36	74.41	S_{11}	192.59	69.54	208.15	86.59
aug-cc-pVDZ			114.72	131.45	94.34	72.30		234.59	74.48	256.50	92.52
d-aug-cc-pVDZ			116.88	130.21	96.42	71.17					
cc-pVDZ		(C_{2v}, $^3B_2$)	84.14	91.19	71.97	68.42	S_{12}	209.40	94.35	225.56	114.46
aug-cc-pVDZ			103.08	86.78	93.15	64.55		254.75	100.15	277.82	122.17
d-aug-cc-pVDZ			104.65	86.59	95.07	64.09					
cc-pVDZ		(C_{2h}, ^1A_g)	129.92	155.55	86.69	87.55					
aug-cc-pVDZ			156.18	155.26	111.39	85.58					
d-aug-cc-pVDZ			158.33	155.45	113.66	85.16					
cc-pVDZ		(D_{2h}, ^1A_g)			71.71	71.16					
aug-cc-pVDZ					93.29	67.70					
d-aug-cc-pVDZ					95.35	66.74					

[a] All the calculations are carried out on the B3LYP/cc-pVDZ geometry.

Figure 5 as mean dipole polarizability per atom ⟨α⟩/*n*. It can be seen that the effect of diffuse functions on ⟨α⟩ is noticeable. ⟨α_n⟩/*n* uniformly increases by about 25% along the series on passing from the cc-pVDZ to the aug-cc-pVDZ basis set. Further addition of diffuse s, p, and d functions (d-aug-cc-pVDZ basis) has a modest effect. The presence of higher angular f functions

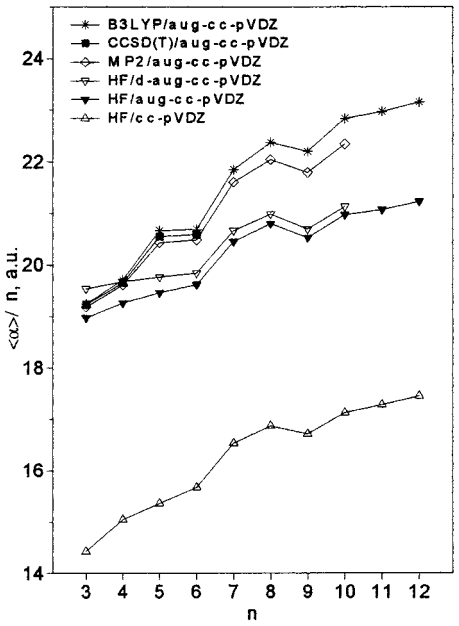

Figure 5. Mean dipole polarizability per atom as a function of the S_n cluster size.

(aug-cc-pVTZ basis) has very modest effect with respect to the results obtained with the d-aug-cc-pVDZ basis. The results indicate that, contrary to what has been observed in oligomeric compounds,[61] in the present case a constant level of theory is necessary through the series.

In the ring structures, the effect of the electron correlation on $\langle\alpha\rangle$ is positive (compare the results in Tables 3 and 4), the increment being within 10%. In the open structures, it is negative and, in S_4, rather large. The D_{2h} conformer of S_4 is a difficult case. It is a pseudoclosed structure, where two S_2 fragments are held together by weak S−S interactions ($r_{1-4} = 2.604$ Å, Table 1). For this structure, we were unable to obtain reliable HF and MP$_n$ polarizability values. Negative contributions to the polarizability in the open structures may be traced back to the presence of low-lying unoccupied p orbitals available in the correlated wave function for charge polarization.[62] It is of interest to note that MP2 and B3LYP calculations give results very close to the CCSD(T) ones. Similarly the comparison between CCSD and CCSD(T) data shows that the effect of the triple substitution is quite small. As a conclusion, it can be stated that *the B3LYP/aug-cc-pVDZ level of theory accurately describes the static polarizability of cyclic sulfur clusters*. Note that the present ab initio values for S_8 and S_{12} are 66% and 60% higher, respectively, than the MNDO ones.[27]

The simplest model for the polarizability of a spherical cluster of size n assumes that α can be taken as proportional to the cluster volume, V.[63] This relation was applied to metal[63a,64−67] and Si clusters.[68] Figure 6 illustrates that also cyclic S_n clusters follow the model; thus, α_{Sn} increases monotonically with n and describes a surface area proportional to n. The linear correspondence between $\langle\alpha\rangle$ and V, within the theory of atoms in molecules, was pointed out previously.[69,70]

$\langle\alpha\rangle/n$ increases with the cluster size at all the levels of theory showing some even−odd oscillation and reaching an extrapolated limit value of 25.4 and 26.1 au at MP2/aug-cc-pVDZ//B3LYP/cc-pVDZ and B3LYP/aug-cc-pVDZ//B3LYP/cc-pVDZ, respectively, the same extrapolation procedure being used as before: $\alpha_n/n = a + b/n + c/n^2$. These figures can be compared with the bulk value of 28.1 au per atom estimated from the Clausius−Mosotti relation

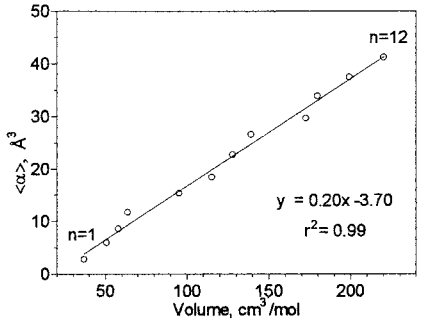

Figure 6. Mean dipole polarizability of the S_n cluster as a function of the cluster volume. The computed volume corresponds to the 0.001 au density contour. Theory is B3LYP/aug-cc-pVDZ//B3LYP/cc-pVDZ.

$$\langle\alpha\rangle_{\text{bulk}} = \frac{3}{4\pi}\left(\frac{\epsilon - 1}{\epsilon + 2}\right)V_{\text{at}}$$

where ϵ is the dielectric constant of the sublimed S (3.69)[1] and V_{at} is the volume of the S atom evaluated as 36.8 cm^3/mol by B3LYP/aug-cc-pVDZ calculations. It is of interest to note that the $\langle\alpha\rangle_{\text{bulk}}$ value of S is very close to the corresponding value for Si of 24−25 au.[68,71,72]

Figure 5 shows that static S_n polarizabilities have $\langle\alpha\rangle/n$ values below the predicted bulk limit unlike what happens in metallic,[73] small Si_n, Ge_n, Ga_nAs_m,[72] and II−VI semiconductor clusters,[74] for which $\langle\alpha\rangle/n$ decreases with the cluster size and the bulk limit is reached from above. On the contrary in large Si_n clusters ($60 < n < 120$), the mean observed cluster polarizabilities are smaller than the bulk value.[72] This was ascribed to size dependence of the dielectric constant due to quantum size effects. In polisylane[75] and π-conjugated polyene[76] compounds $\langle\alpha_n\rangle/n$ usually increases with n, although examples are also reported in the literature showing that in some donor−acceptor substituted polyenes α_n/n vs n decreases as well as increases with the polyene chain length, depending on the donor−acceptor substituent.[77] These findings suggest that the size dependence of $\langle\alpha_n\rangle$ is not straightforward.

Within the two-state model, the molecular polarizability is essentially related to the HOMO−LUMO energy gap. The variation along the series of the HF HOMO−LUMO energy gap, as well as the HF and B3LYP IP − EA values, evaluated through a ΔSCF procedure from the total energies of the neutral molecule and the ion, is reported in Figure 7. The comparison with the results in Figure 5 shows that no clear correlation exists between the HOMO−LUMO gap and α_n/n, suggesting that the cluster hardness is not the leading factor for the polarizability evolution in the homocyclic sulfur clusters. In addition, no relation is found between α_n/n and the lowest electronic transition energy and/or the transition moment, as evaluated by TD-B3LYP/aug-cc-pVDZ//B3LYP/cc-pVDZ calculations. A simple two-state model thus appears to be not applicable.

The interplay between polarizability, hardness, and chemical stability has suggested that for the generic reaction $A_mB_n \rightarrow mA + nB$ a linear relationship can be established between the change in dipole polarizability $\delta\alpha$ and the bond dissociation energy:[5,79]

$$D = A + B\delta\alpha$$

where B is a positive term, which implies that, in agreement with the MPP, $\alpha_{A_mB_n} < m\alpha_A + n\alpha_B$. For the atomization reaction $S_n \rightarrow n$S, we have an opposite behavior with $\alpha_n > n\alpha_1$. We attribute this behavior to the particular electronic structure of the clusters containing many mutually interacting lone-pairs.

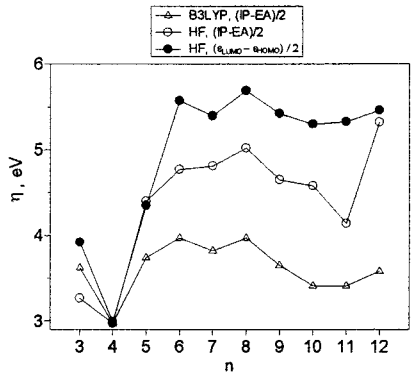

Figure 7. S_n hardness as a function of the S_n cluster size. Basis set is aug-cc-pVDZ.

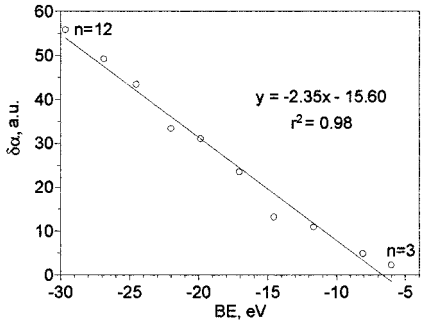

Figure 8. Difference polarizability, $\delta\alpha = \langle\alpha_M\rangle - n\langle\alpha_1\rangle$, as a function of the atomization energy of the S_n cluster. Theory is B3LYP/aug-cc-pVDZ//B3LYP/cc-pVDZ.

Indeed, as was clearly expressed by Dykstra et al.,[78] "in a point−multipole distribution a dipole induced at one point by an external field will augment the field experienced at a neighboring point". As a consequence " the net dipole polarizability of the distribution will be greater than the sum of the α's from the points". This is thought to happen in the present case. Obviously, the comparison between α_n and $n\alpha_1$ sees the polarizability in terms of additive contributions of the individual fragments. Nonadditivity should imply incorporating intramolecular polarization.[80] To validate this point, we constructed difference density maps, $\Delta\rho = \rho_M - \rho$(atoms), in the planar S_3 and S_4 C_{2v} structures. Figure 9 clearly shows, besides the expected concentration of charge in the bonding region, a strong electron transfer from the atoms to the outside of the cluster, indicating that the lone-pair density in the molecule is more diffuse and hence more polarizable than in the free atom. Clearly, in a situation where the polarizability increment due to mutual polarization is not more than balanced by a polarizability decrease owing to bond formation, the MPP cannot hold. Thus, although the atomization energy of S_n increases with n, the polarizability difference $\langle\alpha_M\rangle - \sum_i\langle\alpha_i\rangle$ may also increase with n (Figure 8). In the circumstance, difference polarizability $\delta\alpha$ is expected to increase with the number of the valence electrons, N. Figure 10 shows that $\delta\alpha$ and N are linearly related. Furthermore, the difference polarizability per atom, $\delta\alpha/n$, also linearly increases with N ($r^2 = 0.95$), indicating that, not unexpectedly, mutual polarization interactions become progressively stronger.

It is of interest to note that $\sum_i\langle\alpha_i\rangle$ is found to be smaller than $\langle\alpha_M\rangle$ in other lone-pair rich compounds such as the F_2, Cl_2, Br_2, I_2, O_2,[6] O_3,[81] and in Be_n,[82] As_4,[83] and linear diradical carbon clusters.[84]

The anisotropy of the polarizability is related to the particular structure of the cluster. For a given cluster, $\Delta\alpha$ is a minimum

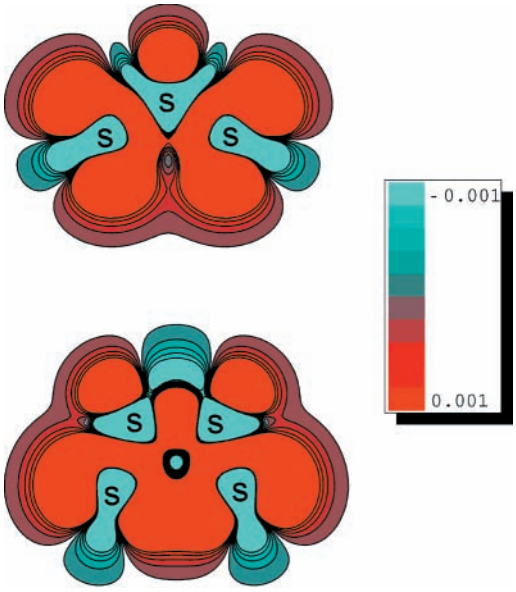

Figure 9. Differential electronic density maps $\Delta\rho = \rho_M - \rho$(atoms) for S_3-C_{2v}-$^1A_1$ and S_4-C_{2v}-$^1A_1$ structures in a plane 0.5 Å above the molecular plane. Theory is B3LYP/aug-cc-pVDZ//B3LYP/cc-pVDZ.

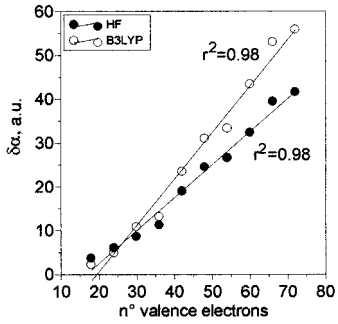

Figure 10. Difference polarizability, $\delta\alpha = \langle\alpha_M\rangle - n\langle\alpha_1\rangle$, as a function of the number of the valence electrons in the S_n cluster. Basis set is aug-cc-pVDZ.

for the most compact structure (compare, for example, $\Delta\alpha$ of the S_3 and S_4 isomers in Table 3). It shows a clear even−odd alternation, the odd cluster being less anisotropic and hence more compact.

3.3. Dipole Moment and Vibrational Effects. The experimental gas-phase $\langle\alpha\rangle$ value includes contributions from dispersion, vibrational, and, for molecules with a permanent dipole moment, dipole orientation effects. Dynamic $\langle\alpha\rangle$ values are here not considered, while, to account for dipole rotation effects, assuming that the molecular system can be freely aligned along the external field, the total effective polarizability can be expressed as

$$\langle\alpha_{eff}\rangle = \langle\alpha\rangle + \frac{\mu^2}{3kT}$$

where μ is the static dipole moment of the cluster. Calculated B3LYP/aug-cc-pVDZ//B3LYP/cc-pVDZ values of μ are μS_3-C_{2v} ($^1A_1$) = 0.56 D, μS_5 = 0.39 D, μS_7 = 0.16 D, μS_9 = 0.13 D, and μS_{11} = 0.13 D, while cyclic even-membered clusters are apolar by symmetry. At room temperature, under thermal equilibrium, these numbers lead to negligible dipole-rotating effect, except for S_5, in which its contribution amounts to ca. 10%.

Pure vibrational contributions to $\langle\alpha\rangle$ are reported in Table 5. It can be seen that at the HF level they are significant only for

TABLE 5: Electronic and Vibrational Contributions to the Static Polarizability of S_n Cluster

			HF//HF		B3LYP//B3LYP
		basis set	$\langle\alpha\rangle^e$	$\langle\alpha\rangle^v$	$\langle\alpha\rangle^v$
S_2		cc-pVDZ	29.39	0.00	0.00
		aug-cc-pVDZ	41.07	0.00	
S_3	(D_{3h}, $^1A_{1'}$)	cc-pVDZ	41.80	0.11	0.05
		aug-cc-pVDZ	55.42	0.08	
	(C_{2v}, $^1A_1$)	cc-pVDZ	52.78	3.97	2.36
		aug-cc-pVDZ	60.07	4.61	
	(C_{2v}, $^3A_2$)	cc-pVDZ	55.63	14.73	0.40
		aug-cc-pVDZ	70.57	15.39	
S_4	(C_{2v}, $^1A_1$)	cc-pVDZ	82.22	10.93	5.26
		aug-cc-pVDZ	102.18	11.30	
S_5		cc-pVDZ	73.77	13.94	4.04
		aug-cc-pVDZ	94.08	11.60	
S_6		cc-pVDZ	90.68	0.90	1.25
		aug-cc-pVDZ	113.92	0.78	
S_7		cc-pVDZ	109.72	1.63	2.82
		aug-cc-pVDZ	136.73	1.77	
S_8		cc-pVDZ	129.15	1.43	2.83
		aug-cc-pVDZ	159.66	1.47	
S_9		cc-pVDZ	143.78	1.93	2.79
S_{10}		cc-pVDZ	163.27	1.78	3.52
S_{11}		cc-pVDZ	180.93	2.00	3.54
S_{12}		cc-pVDZ	198.65	1.98	3.13

the lower terms ($n = 5$), for which the most contributing vibrational modes are of stretching type. For $6 \leq n \leq 12$, $\langle\alpha\rangle^v$ is negligible, being associated with ring deformation modes of very low intensity. Inclusion of diffuse functions changes little $\langle\alpha\rangle^v$, contrary to $\langle\alpha\rangle^e$, which substantially increases. In the smaller clusters ($n \leq 5$), electron correlation decreases $\langle\alpha\rangle^v$, which makes negligible its contributions also in these compounds. For $n > 6$, electron correlation increases $\langle\alpha\rangle^v$, which remains, however, a small fraction of $\langle\alpha\rangle^e$. Therefore, inclusion of the vibrational contributions does not change the above results and considerations.

On passing, the comparison between the HF results in Tables 4 and 5 allows estimation of the effect of the geometry on $\langle\alpha\rangle^e$: the use of nonequilibrium geometry makes $\langle\alpha\rangle^e$ increase by ca. 5%.

Conclusions

The objective of the work was a description, by the aid of quantum chemical computations, of the size dependence of structural and electronic properties of mainly cyclic sulfur clusters, such as ground-state geometry, relative stability, HOMO−LUMO energy gap, and polarizability. DFT-B3LYP methodology has been revealed to be suitable to this end, by producing results in excellent agreement with experimental data, where available, and with those obtained by much more sophisticated post-HF procedures such as CCSD(T) methods. Compact cyclic S_n structures are characterized by a rapid convergence of the average bond length and binding energy per atom to the asymptotic limit for $n \rightarrow \infty$. The mean dipole polarizability monotonically increases with n, well describing the surface area of the spherical cluster. The mean dipole polarizability per atom increases with n and approaches the bulk limit from below as in the case of large Si_n clusters, but contrary to small semiconductor and metallic clusters. The $\langle\alpha_n\rangle/n$ evolution cannot be rationalized in terms of a two-state model. It is suggested that the peculiar behavior of the sulfur cluster polarizability is dominated by the presence of lone-pairs and their mutual interaction, which determines $\langle\alpha_M\rangle$ to be greater than $\sum_i\langle\alpha_i\rangle$. The sulfur clusters represent a clear example in which the MPP principle does not hold. Pure vibrational effects on $\langle\alpha\rangle$ are negligible in dependence of low-intensity vibrational transitions.

Acknowledgment. This work was partially supported by MURST, Rome.

References and Notes

(1) Miller, T. M. *CRC Handbook of Chemistry and Physics*, 77th ed.; CRC Press: Boca Raton, FL, 1996−1997. Bonin, K. D.; Kresin, V. U. *Electric-dipole polarizabilities of atoms, molecules and clusters*; World Scientific: London, 1997.

(2) Minkin, V. I. *Pure Appl. Chem.* **1999**, *71*, 1919.

(3) Chattaraj, P. K.; Segupta, S. *J. Phys. Chem.* **1996**, *100*, 16126.

(4) Ghanty, T. K.; Ghosh, S. K. *J. Phys. Chem.* **1996**, *100*, 12295.

(5) Hohm, U. *J. Phys. Chem. A* **2000**, *104*, 8418.

(6) Pearson, R. G. *Acc. Chem. Res.* **1993**, *26*, 250.

(7) Chattaraj, P. K.; Fuentealba, P.; Jaque, P.; Toro-Labbé, A. *J. Phys. Chem. A* **1999**, *103*, 9307.

(8) Gutiérrez-Oliva, S.; Jaque, P.; Toro-Labbé, A. *J. Phys. Chem. A* **2000**, *104*, 8955.

(9) Chattaraj, P. K.; Pérez, P.; Zevallos, J.; Toro-Labbé, A. *J. Phys. Chem. A* **2001**, *105*, 4272.

(10) Kar, T.; Scheiner, S. *J. Phys. Chem.* **1995**, *99*, 8121.

(11) Perez, P.; Toro-Labbé, A. *J. Phys. Chem. A* **2000**, *104*, 1557.

(12) Ghanty, T. K.; Ghosh, S. K. *J. Phys. Chem. A* **2000**, *104*, 2975.

(13) Doerksen, R. J.; Thakkar, A. J. *J. Phys. Chem. A* **1999**, *103*, 2141.

(14) Pal, S.; Chandra, A. K. *J. Phys. Chem.* **1995**, *99*, 13865.

(15) Fuentealba, P.; Simòn-Manso, Y.; Chattaray, K. *J. Phys. Chem. A* **2000**, *104*, 3185.

(16) Simòn-Manso, Y.; Fuentealba, P. *J. Phys. Chem. A* **1998**, *102*, 2029. Fuentealba, P.; Reyes, O. *J. Phys. Chem. A* **1999**, *103*, 1376. Fuentealba, P.; Reyes, O. *J. Mol. Struct. THEOCHEM* **1993**, *282*, 65. Toufar, H.; Nulens, K.; Janssens, G. O. A.; Schoonheydt, R. A.; De Proft, F.; Geerlings, P. *J. Phys. Chem.* **1996**, *100*, 15383. Chattaraj, P. K.; Nat, S.; Sannigrahi, A. B. *J. Phys. Chem.* **1994**, *98*, 9143. Hati, S.; Datta, B.; Datta, D. *J. Phys. Chem.* **1996**, *100*, 19808. Ghanty, T. K.; Ghosh, S. K. *J. Phys. Chem.* **1994**, *98*, 9197; **1996**, *100*, 12295; **1996**, *100*, 17429. Roy, R.; Chandra, A. K.; Pal, S. *J. Phys. Chem.* **1994**, *98*, 10447. Segre de Giambiagi, M.; Giambiagi, M. *J. Mol. Struct. THEOCHEM* **1993**, *288*, 273. Politzer, P. *J. Chem. Phys.* **1987**, *86*, 1072. Vela, A.; Gazquez, J. L. *J. Am. Chem. Soc.* **1989**, *112*, 1490. Sicilia, E.; Russo, N.; Mineva, T. *J. Phys. Chem. A* **2001**, *105*, 442. Parr, R. G.; Yang, W. *Annu. Rev. Phys. Chem.* **1995**, *46*, 701. Liu, G. H.; Parr, R. G. *J. Chem. Phys.* **1997**, *106*, 5578. Datta, D. *J. Phys. Chem.* **1992**, *96*, 2409. Pal, N.; Vaval, N.; Roy, S. *J. Phys. Chem.* **1993**, *97*, 4404.

(17) Millefiori, S.; Alparone, A. *J. Mol. Struct. THEOCHEM* **1998**, *431*, 59.

(18) Millefiori, S.; Alparone, A. *Chem. Phys. Lett.* **2000**, *332*, 175.

(19) Millefiori, S.; Alparone, A. *Phys. Chem. Chem. Phys.* **2000**, *2*, 2495.

(20) Millefiori, S.; Alparone, A.; Millefiori, A. *J. Chem. Res., Synop.* **1999**, 239.

(21) Meyer, B. *Chem. Rev.* **1976**, *76*, 567.

(22) Steudel, R.; Albertsen, J.; Zink, K. *Ber. Bunsen-Ges. Phys. Chem.* **1989**, *93*, 502.

(23) Hohl, D.; Jones, R. Q.; Car, R.; Parrinello, M. *J. Chem. Phys.* **1988**, *89*, 6823.

(24) Raghavachari, K.; Rohlfing, C. M.; Binkley, J. S. *J. Chem. Phys.* **1990**, *93*, 5862.

(25) Quelch, G. E.; Schaefer, H. F., III; Mardsen, C. J. *J. Am. Chem. Soc.* **1990**, *112*, 8719 and references therein.

(26) Cioslowski, J.; Szarecka, A.; Moncrieff, D. *J. Phys. Chem.* **2001**, *105*, 501.

(27) Raptis, S. G.; Nasiou, S. M.; Demetropoulos, I. N.; Papadopoulos, M. G. *J. Comput. Chem.* **1998**, *19*, 1698.

(28) Frisch, M. J.; Trucks, G. W.; Schlegel, H. B.; Scuseria, G. E.; Robb, M. A.; Cheeseman, J. R.; Zakrzewski, V. G.; Montgomery, J. A., Jr.; Stratmann, R. E.; Burant, J. C.; Dapprich, S.; Millam, J. M.; Daniels, A. D.; Kudin, K. N.; Strain, M. C.; Farkas, O.; Tomasi, J.; Barone, V.; Cossi, M.; Cammi, R.; Mennucci, B.; Pomelli, C.; Adamo, C.; Clifford, S.; Ochterski, J.; Petersson, G. A.; Ayala, P. Y.; Cui, Q.; Morokuma, K.; Malick, D. K.; Rabuck, A. D.; Raghavachari, K.; Foresman, J. B.; Cioslowski, J.; Ortiz, J. V.; Stefanov, B. B.; Liu, G.; Liashenko, A.; Piskorz, P.; Komaromi, I.; Gomperts, R.; Martin, R. L.; Fox, D. J.; Keith, T.; Al-Laham, M. A.; Peng, C. Y.; Nanayakkara, A.; Gonzalez, C.; Challacombe, M.; Gill, P. M. W.; Johnson, B. G.; Chen, W.; Wong, M. W.; Andres, J. L.; Head-Gordon, M.; Replogle, E. S.; Pople, J. A. *Gaussian 98*, revision A.7; Gaussian, Inc.: Pittsburgh, PA, 1998.

(29) Woon, D. E.; Dunning, T. H. *J. Chem. Phys.* **1994**, *100*, 2975.

(30) Kurtz, H. A.; Stewart, J. J. P.; Dieter, K. M. *J. Comput. Chem.* **1990**, *11*, 82.
(31) Bishop, D. M.; Kirtman, B. *J. Chem. Phys.* **1991**, *95*, 2646; *J. Chem. Phys* **1992**, *97*, 5255.
(32) Huber, K. P.; Herzberg, G. *Molecular Spectra and Molecular Structure. IV. Constants of Diatomic Molecules*; Van Nostrand Reinhold: New York, 1974.
(33) Bash, H. *Chem. Phys. Lett.* **1989**, *157*, 129.
(34) Salahub, D. R.; Foti, A. E.; Smith, V. H., Jr. *J. Am. Chem. Soc.* **1978**, *100*, 7847.
(35) Rice, J. E.; Amos, R. D.; Handy, N. C.; Lee, T. J.; Schaefer, H. F., III. *J. Chem. Phys.* **1986**, *85*, 963.
(36) Zakrzewski, V. G.; von Niessen, W. *Theor. Chim. Acta* **1994**, *88*, 75.
(37) Koch, W.; Natterer, J.; Heinemann, C. *J. Chem. Phys.* **1995**, *102*, 6159.
(38) Goddard, J. D.; Chen, X.; Orlova, G. *J. Phys. Chem.* **1999**, *103*, 4078.
(39) Fueno, T.; Buenker, R. J. *Theor. Chim. Acta* **1988**, *73*, 123.
(40) Nimlos, N. M.; Ellison, G. B. *J. Phys. Chem.* **1986**, *90*, 2574.
(41) Berkowitz, J.; Lipschitz, C. *J. Chem. Phys.* **1968**, *48*, 4346.
(42) Meyer, B.; Spitzer, K. *J. Phys. Chem.* **1972**, *76*, 2274.
(43) Lenain, P.; Picquenard, E.; Lesne, J. L.; Corset, J. *J. Mol. Struct.* **1986**, *142*, 355.
(44) Brabson, G. D.; Mielke, Z.; Andrews, L. *J. Phys. Chem.* **1991**, *95*, 79. Assanzadeh, P.; Andrews, L. *J. Phys. Chem.* **1992**, *96*, 6579.
(45) Von Niessen, W. *J. Chem. Phys.* **1991**, *95*, 8301.
(46) Hunsicker, S.; Jones, R. O.; Gauteför, G. *J. Chem. Phys.* **1995**, *102*, 5917.
(47) Abboud, J.-L.; Esseffar, M.; Herreros, M.; Mó, O.; Molina, M. T.; Notario, R.; Yáñez, M. *J. Phys. Chem.* **1998**, *102*, 7996.
(48) Orlova, G.; Goddard, J. D. *J. Phys. Chem.* **1999**, *103*, 6825.
(49) Steidel, J.; Pickardt, J.; Steudel, R. *Z. Naturforsch.* **1978**, *33B*, 1554.
(50) Steudel, R.; Steidel, J.; Pickardt, J.; Schuster, F.; Reinhardt, R. *Z. Naturforsch.* **1980**, *35B*, 1378.
(51) Rettig, S. J.; Trotter, J. *Acta Crystallogr.* **1987**, *C43*, 2260.
(52) Steudel, R.; Steidel, J.; Reinhardt, R. *Z. Naturforsch.* **1983**, *38B*, 1548.
(53) Steidel, J.; Steudel, R. *J. Chem. Soc., Chem. Commun.* **1982**, 1312.
(54) Steidel, J.; Steudel, R.; Kutoglu, A. *Z. Anorg. Allg. Chem.* **1981**, *476*, 171.
(55) Sieck, A.; Porezag, D.; Frauenheim, Th.; Pederson, M. R.; Jackson, K. *Phys. Rev. A* **1997**, *56*, 4890.
(56) Moore, C. E. *Atomic Energy Levels*; NSRDS Nat. Stand. Ref. Data Serv. Circ. No. 35; U.S. National Bureau of Standards, CPO: Washington, D.C., 1969. Raghavachari, K. *J. Chem. Phys.* **1986**, *84*, 5672.
(57) Nagaya, K.; Hayakawa, J.; Yao, M. *Trans. Mater. Res. Soc. Jpn.* **1996**, *20*, 404.
(58) Das, A. K.; Thakkar, A. J. *J. Phys. B: At. Mol. Opt. Phys.* **1998**, *31*, 2215.
(59) Meyer, B.; Oommen, T. V.; Jensen, D. *J. Phys. Chem.* **1971**, *75*, 912. Meyer, B.; Stroyer-Hansen, T.; Jensen, D.; Oommen, T. V. *J. Am. Chem. Soc.* **1971**, *93*, 1034.
(60) Stiehler, J.; Hinze, J. *J. Phys. B: At. Mol. Opt. Phys.* **1995**, *28*, 4055.
(61) Hurst, G. J. B.; Dupuis, M.; Clementi, E. *J. Chem. Phys.* **1988**, *89*, 385. Champagne, B.; Mosley, D. H.; André J.-M. *J. Chem. Phys.* **1994**, *100*, 2034.
(62) Werner, H.-J.; Meyer, W. *Phys Rev. A* **1976**, *13*, 13.
(63) (a) Moullet, I.; Martines, J. L.; Reuse, F.; Buttet, *J. Phys. Rev. B* **1990**, *42*, 11598 and references therein. (b) Brink, T.; Murray, J. S.; Politzer, P. *J. Phys. Chem.* **1993**, *98*, 4305.
(64) Rayane, D.; Allouche, A. R.; Benichou, E.; Antoine, R.; Aubert-Frecon, M.; Dugourd, Ph.; Broyer, M.; Ristori, C.; Chandezon, F.; Huber, B. A.; Guet, C. *Eur. Phys. J. D* **1999**, *9*, 243.
(65) Rubio, A.; Alonso, J. A.; Blase, X.; Balbás, L. C.; Louie, S. G. *Phys. Rev. Lett.* **1996**, *77*, 247.
(66) Hati, S.; Datta, D. *J. Phys Chem.* **1994**, *98* 10451; **1995**, *99*, 10742.
(67) Ghanty, T. K.; Ghosh, S. K. *J. Phys. Chem.* **1993**, *97*, 4951.
(68) Jackson, K.; Pederson, M.; Wang, C.-Z.; Ho, K.-M. *Phys. Rev. A* **1999**, *59*, 3685.
(69) Gough, K. M. *J. Chem. Phys.* **1989**, *91*, 2424.
(70) Laidig, K. E.; Bader, R. F. W. *J. Chem. Phys.* **1990**, *93*, 7213.
(71) Vasiliev, I.; Ogut, S.; Chelikowsky, R. *Phys. Rev. Lett.* **1997**, *78*, 4805.
(72) Schafer, R.; Schlecht, S.; Woenckhaus, J.; Becker, J. A. *Phys. Rev. Lett.* **1996**, *76*, 471.
(73) Calaminici, P.; Köster, A. M.; Vela, A. *J. Chem. Phys.* **2000**, *113*, 2199. Calaminici, P.; Jug, K.; Köster, A. M. *J. Chem. Phys.* **1999**, *111*, 4613.
(74) Troparevsky, M. C.; Chelikowsky, J. R. *J. Chem. Phys.* **2001**, *114*, 943.
(75) Kirtman, B.; Hasan, M. *J. Chem. Phys.* **1992**, *96*, 470. Champagne, B.; Perpete, E.; André, J.-M.; Kirtman, B. *J. Chem. Soc., Faraday Trans.* **1995**, *91*, 1641.
(76) Dalskov, E. K.; Oddershede, J.; Bishop, D. M. *J. Chem. Phys.* **1998**, *108*, 2152. Hamada, T. *J. Chem. Soc., Faraday Trans.* **1996**, *92*, 3165.
(77) Tretiak, S.; Chernyak, V.; Mukamel, S. *Chem. Phys. Lett.* **1999**, *245*, 145.
(78) Stout, J. M.; Dykstra, C. E. *J. Am. Chem. Soc.* **1995**, *117*, 5127. Zhou, T.; Dykstra, C. E. *J. Phys. Chem. A* **2000**, *104*, 2204.
(79) Hohm, U. *J. Chem. Phys.* **1994**, *101*, 6362.
(80) Applequist, J.; Carl, J.-R.; Fung, K.-K. *J. Am. Chem. Soc.* **1972**, *94*, 2952.
(81) Maroulis, G. *J. Chem. Phys.* **1999**, *111*, 6846.
(82) Begué, D.; Pouchan, C. *J. Comput. Chem.* **2001**, *22*, 230.
(83) Hohm, U.; Goebel, D.; Karamanis, P.; Maroulis, G. *J. Phys. Chem.* **1998**, *102*, 1237.
(84) Fuentealba, P. *Phys. Rev. A* **1998**, *58*, 4232.